

Stress and Strain in Flat Piling of Disks

Shio Inagaki* and James T. Jenkins

*Department of Theoretical and Applied Mechanics
Cornell University, Ithaca, NY 14853 USA*

(Received)

We have created a flat piling of disks in a numerical experiment using the Distinct Element Method (DEM) by depositing them under gravity. In the resulting pile, we then measured increments in stress and strain that were associated with a small decrease in gravity. We first describe the stress in terms of the strain using isotropic elasticity theory. Then, from a micro-mechanical view point, we calculate the relation between the stress and strain using the mean strain assumption. We compare the predicted values of Young's modulus and Poisson's ratio with those that were measured in the numerical experiment.

KEYWORDS: granular piling, stress-strain relation, Distinct Element Method

1. Introduction

The ultimate goal of our research is to describe how stresses propagate through granular media. Physical experiments¹⁾ indicate that when a localized force is applied at a surface of a layer of sand, the stress distribution on the bottom of the layer depends on how the layer was constructed. The pressure distribution under a conical sand pile also depends on the way the pile was built and may have a local minimum under the apex of a pile.^{2,3)} We don't yet know how to describe the way that stress propagates through a pile or how the propagation depends on its construction history.

In this paper, as a first step, we focus on a two-dimensional example with possible anisotropy in the vertical direction: a flat pile of circular, elastic, frictional disks, deposited under gravity onto a frictional, flat base. In this case, as shown in § 4.3, we find that the anisotropy due to the gravity is small enough to neglect. In § 2, we write down equations of force balance, assuming that the pile is continuous body, in order to predict stress and strain within it. Assuming that the pile is an isotropic elastic body, these equations are solved exactly. But the problem is that material constants, such as the Young's modulus and Poisson's ratio are unknown. In the next

* E-mail address: shio@mail.ne.jp, Present Address: Department of Basic Science, University of Tokyo, Komaba, Tokyo 153-8902, Japan

chapter, we adopt the mean strain assumption in order to predict the material constants of an assembly of disks in terms of micro-scopic material properties, such as the contact stiffness. Here, a relationship between the micro-scopic and macro-scopic material properties is obtained. In § 4 we build a flat pile with elastic, frictional circular disks in a numerical experiment using the Distinct Element Method, a kind of molecular dynamics. Then, the stress and strain in the pile are measured in a deformation produced by reducing gravity, and the predictions that are made in § 3 are tested against the measured values. In the last chapter, we discuss the reasons for the differences between the predictions based on the mean strain assumption and the measured results and indicate what more should be done.

2. Elasticity theory

2.1 Continuum theory

The equation of motion for a granular piling is written as

$$\frac{\partial \sigma_{ij}}{\partial x_j} + \rho b_i = \rho a_i,$$

where σ_{ij} is the stress, ρ is the mass density, b_i is the body force per unit area, and a_i is the acceleration. In this paper, we focus on only a two-dimensional case, so the summation should be taken from 1 to 2. The body force is gravity having only a vertical component, $b_2 = -g$.

We are interested in a static piling, so $a_i = 0$, $i = 1, 2$. The equilibrium equations for the two-dimensional case are

$$\frac{\partial \sigma_{11}}{\partial x_1} + \frac{\partial \sigma_{12}}{\partial x_2} = 0, \quad (1)$$

$$\frac{\partial \sigma_{12}}{\partial x_1} + \frac{\partial \sigma_{22}}{\partial x_2} - \rho g = 0. \quad (2)$$

The boundary conditions are defined for a pile of uniform height h : the horizontal boundary is periodic and, at the free surface, the shear stresses and the vertical stress are zero, $\sigma_{22}(x_2 = h) = 0$ and $\sigma_{12}(x_2 = h) = 0$. Then, by symmetry $\sigma_{12} \equiv 0$. By solving eqs. (1) and (2), the components of stresses are

$$\sigma_{11} = \sigma_{11}(x_2), \quad (3)$$

$$\sigma_{22} = \rho g(x_2 - h). \quad (4)$$

In these equations, σ_{11} is indeterminate, so the exact solutions can not be obtained using only this information. In the next section, we will adopt isotropic elasticity theory in order to obtain an exact determination of σ_{11} .

2.2 Isotropy

The horizontal and vertical strains, E_{11} and E_{22} , can be obtained by introducing the constitutive relations of isotropic elasticity:

$$E_{11} = \frac{1}{E}(\sigma_{11} - \nu\sigma_{22}), \quad (5)$$

$$E_{22} = \frac{1}{E}(\sigma_{22} - \nu\sigma_{11}), \quad (6)$$

where ν is Poisson's ratio and E is Young's modulus.

The horizontal stress, σ_{11} , given by eq. (3), is obtained using eq. (5) and requiring that $E_{11} \equiv 0$ because of the horizontal periodic boundary condition. Then

$$\begin{aligned} \sigma_{11} &= \nu\sigma_{22} \\ &= \nu\rho g(x_2 - h). \end{aligned} \quad (7)$$

Substituting eqs (4) and (7) into eq. (6), the vertical strain is

$$\begin{aligned} E_{22} &= \frac{1 - \nu^2}{E}\sigma_{22} \\ &= \frac{1 - \nu^2}{E}\rho g(x_2 - h). \end{aligned} \quad (8)$$

3. Prediction of the material constants

From a micro-mechanical view point, the average stress can be written using an orientational distribution of contacts, $D(\mathbf{n})$, and a contact force, \mathbf{f}^c , as

$$\sigma_{ij} = \frac{\gamma}{\pi a} \int D(\mathbf{n}) f_i^c n_j d\Omega,$$

where γ is the area fraction of the disks, a is a radius of disk, \mathbf{n} is the unit vector from the center of the disk to a contact, and $d\Omega$ is the element of contact angle.

Here, we make the strong assumption that the contact displacement is determined by the average strain as

$$u_p = aE_{pq}n_q.$$

Then, the contact force is also determined by the average strain as

$$\begin{aligned} f_i^c &= K_{ip}u_p \\ &= K_{ip}aE_{pq}n_q, \end{aligned}$$

where

$$K_{ip} = K_N n_i n_p + K_T (\delta_{ip} - n_i n_p),$$

in which K_N and K_T are normal and tangential stiffness, respectively.

We assume that the orientational distribution of contact is isotropic; then

$$D(\mathbf{n}) = \frac{k}{2\pi}, \quad (9)$$

where k is the average number of contacts per disk.¹⁰⁾ As shown in § 4.3, it is appropriate to assume that the contact angle distribution is isotropic.

Then,

$$\sigma_{ij} = \frac{\gamma}{\pi a} \int \frac{k}{2\pi} a K_{ip} n_q n_j d\Omega E_{pq}. \quad (10)$$

The general form of Hooke's law is

$$\sigma_{ij} = C_{ijpq} E_{pq}. \quad (11)$$

By comparing eqs (10) and (11),

$$C_{ijpq} = \frac{\gamma}{\pi a} \int \frac{k}{2\pi} a K_{ip} n_q n_j d\Omega.$$

After the integration in eq. (11) is carried out, eq. (10) becomes

$$\sigma_{ij} = \frac{\gamma k}{4\pi} [(K_N + K_T) E_{ij} + \frac{1}{2} (K_N - K_T) E_{kk} \delta_{ij}].$$

When the stress is expressed in terms of strain, the coefficients are called Lamé's constants. Now, Lamé's constants are obtained in terms of stiffness of disks as

$$\begin{aligned} 2\mu &= \frac{\gamma k}{4\pi} (K_N + K_T), \\ \lambda &= \frac{\gamma k}{8\pi} (K_N - K_T). \end{aligned}$$

Then Young's modulus, E and Poisson's ratio, ν , are converted from Lamé's constants, so they can also be expressed in terms of stiffness of disks as

$$\begin{aligned} \nu &= \frac{\lambda}{2\mu + \lambda} = \frac{K_N - K_T}{3K_N + K_T}, \\ E &= \frac{4\mu(\mu + \lambda)}{2\mu + \lambda} = \frac{\gamma k}{\pi} \frac{(K_N + K_T) K_N}{3K_N + K_T}. \end{aligned} \quad (12)$$

Using this relation between micro-scopic and macro-scopic material property, we can predict Young's modulus and Poisson's ratio.

4. Numerical experiments

In this paper, we adopt Distinct Element Method (DEM), which was invented by Cundall,⁴⁾ in order to produce deformed granular aggregates in which stress and strain can be measured. We follow the algorithm of A. Shimosaka⁵⁾ and H. Hayakawa.⁶⁾

Using DEM, we make a two-dimensional flat pile that is composed of elastic, frictional, circular disks on a frictional smooth bottom, and measure stress and strain at each point.

4.1 Setting

Elastic, frictional, circular disks are deposited on a flat frictional bottom, layer by layer. Two diameters of disks are chosen that are slightly different from each other, in order to avoid a crystal structure. The horizontal boundary is periodic. We let this pile relax until the disks come to a static state, after dissipating all of their kinetic energy in collisions. (See the left panel of Fig. 1.) There is the possibility of the existence of depositional anisotropy in the vertical direction that will be considered later in § 4.3. The right panel of Fig. 1 shows a Voronoi tessellation of this pile. Voronoi tessellation divides the whole domain into cells using perpendicular bisectors of the lines of centers, so that each cell contains one center, indicated by a dot. Voronoi cells are used to measure strain in a granular assemblies as defined in § 4.2.

The parameters that are used in the actual simulation are normalized so that the maximum disk diameter, the gravitational acceleration, and the mass per unit area are all unity. Consequently, upon taking the summation over all contacts B with disk A , the dimensionless equation of motion for disk A is

$$m'_A \frac{d^2 x'_A}{dt'^2} = \sum_B \left[\eta' \frac{d(x'_B - x'_A)}{dt'} - k'(x'_B - x'_A) \right] - m'_A,$$

where $x = lx'$, $t = \sqrt{l/g} t'$. In our model, contact forces consist of elastic and viscous forces which are linearly proportional to the relative displacement and the relative velocity, respectively. A dash denotes a non-dimensional variable. For example, a dimensionless elastic coefficient and a dimensionless viscous coefficient are calculated as $k' = (l/\bar{m}g)k$ and $\eta' = (1/\bar{m})\sqrt{l/g} \eta$, respectively, where \bar{m} is the mass per unit area and m'_A is the dimensionless mass of disk A . The dimensional parameters used in our calculations are shown in Table I.

4.2 Measurement of stress and strain

There exist several definitions for stress and strain of granular aggregates.⁷⁻⁹⁾ In this paper we adopt a simplified form of definitions,^{7,8)} that are consistent with each other in two

dimensions. After reducing gravity by 10%, we measure the displacements of the disks and the increments of the contact forces and, from them, calculate increments of stress and strain. The increment of the strain at a point at the center of disk A is taken to be

$$\dot{E}_{ij}^A = \frac{\gamma}{\pi a_A^2} \sum_B \dot{u}_i^{AB} n_j^{AB} l^{AB},$$

where γ is the area fraction of the disks, \mathbf{u}^{AB} is a displacement of disk A relative to disk B , \mathbf{n}^{AB} is the unit vector in the direction of contact between disk A and B , and l^{AB} is the length of the side of a Voronoi cell which is shared by cell A and cell B , with the name of a cell the same as the name of a disk which is inside of the cell. The corresponding increment in stress is taken to be

$$\dot{\sigma}_{ij}^A = \frac{\gamma}{\pi a_A} \sum_C \dot{f}_{ci}^{AC} n_j^{AC},$$

where \mathbf{f}_c^{AC} is a contact force exerted on disk A by disk C and a_A is the radius of disk A . In the definition of strain, the summation is taken over all the neighbourings which share sides of Voronoi cells in between; while for stress, the sum is taken over all of the pairs of contacts.

The increments of stress and strain are measured at each disk center according to the definitions above. They are taken to be an average over disks which are included in a horizontal slice with a width of 1.5 dimensionless units at each height. Figure 2 shows the increment of the dimensionless stress versus. the height, normalized by the maximum diameter. It is linearly proportional to the height of the pile due to the weight of the disks.

Now we are interested in the increments of stress and strain associated with reduction of gravity by 10%. Then the increments of stress components are expressed in terms of the increment of gravity, $\delta g = -0.1g$ as

$$\dot{\sigma}_{11} = \nu \dot{\sigma}_{22} \tag{13}$$

$$= \nu \rho \delta g (x_2 - h) \tag{14}$$

and

$$\dot{\sigma}_{22} = \rho \delta g (x_2 - h). \tag{15}$$

The slope of the line along $\dot{\sigma}_{22}$ coincides well with the value, -0.07 , which is estimated from eq.(15), where $\rho = 0.83$ which is calculated from the area fraction. In this respect, the continuous description pictures the stress well.

Figure 3 shows the increment of strain versus. height. From eq.(8), the increment of strain is

$$\dot{E}_{22} = \frac{1 - \nu^2}{E} \dot{\sigma}_{22} \quad (16)$$

$$= \frac{1 - \nu^2}{E} \rho \delta g(x_2 - h). \quad (17)$$

Comparing eq. (17) and Fig. 3, we found that E_{22} is related linearly with the height of the pile with some fluctuation.

Next, let us consider the relation between stress and strain. Figure 4 shows the increment of the dimensionless stress versus the increment of strain. From eq. (16), stress is expected to be linearly proportional to strain. The linear relation can be seen in Fig. 4 between stress and strain in our numerical experiment.

4.3 Contact angle distribution

Figure 5 shows the contact angle distribution. There are peaks around $\pi/3$, $2\pi/3$, and π . It indicates that the disk configuration is nearly a hexagonal packing. Although we expected that there would exist a depositional anisotropy due to the process of construction of the pile, it was found that the contact angle distribution can be assumed to be isotropic in a macroscopic sense. So the assumption that was made in eq.(9) is supported. The hexagonal structure also can be seen in the Voronoi tessellation (see the right panel of the Fig. 1, although it should be noted that a side of Voronoi cells is defined as a bisection of the nodes connected the centers of a pair of disks, but it doesn't mean that they are necessarily in contact as shown by the fact that the average number of contacts is about 4.7.

4.4 Measurement of the material constants

Under the assumption that the material is isotropic, we can characterize its elastic response using only two constants (e.g., the Lamé constants, or Young's modulus and Poisson's ratio). However, we don't yet know such constants for the granular aggregate as a bulk. In other situations involving anisotropy, two constants are not be sufficient to characterize the elasticity of a granular material.

For the isotropic material, we can estimate Young's modulus and Poisson's ratio from eq. (13) and (17) as

$$\nu = \frac{\dot{\sigma}_{11}}{\dot{\sigma}_{22}},$$

$$E = (1 - \nu^2) \frac{E_{22}}{\sigma_{22}}. \quad (18)$$

The ratio of σ_{11} against σ_{22} is almost constant as shown in Fig. 6 except at the surface of the pile. Also, Young's modulus, estimated from eq. (18), is shown in Fig. 5. The fluctuation in Fig. 5 is found is larger than that for Poisson's ratio and may not be negligible.

As predicted in § 3, using $\gamma = 0.83$ and $k = 4.7$, as measured in the numerical simulation, the dimensionless Young's modulus $E' \equiv (l/\bar{m}g)E$ is 9.3×10^3 and the Poisson's ratio is 0.25. We can compare those values with those obtained in the numerical experiments shown in Figs. 6 and 5. The predicted Young's modulus is almost 2.58 times of the measured value; while the predicted Poisson's ratio is half of the measured value. That is, the predicted properties of the pile are stiffer than those measured.

4.5 Fluctuation of strain

In our micro-mechanical view point, fluctuations in the strain were not taken into account. Consequently, the predicted material constants were larger than those measured in the numerical simulation, because the disks in the simulation can translate and rotate in ways different from that predicted by the average strain in order to satisfy force and moment equilibrium. These additional degrees of freedom allows them to behave more flexibly than predicted. Figure 8 shows the fluctuation of strain ($\Delta E_{22}/E_{22}$) versus the height. The fluctuation, ΔE_{22} , is evaluated by the ratio of the absolute value of the deviation from the mean strain to the local value of the mean strain. On average, the strain fluctuation δE_{22} is 65% of the strain itself, except near the bottom and the surface of the pile. The fluctuation of strain is very large, especially near the boundaries. We need to take this fluctuation into account in order to better describe the relation between stress and strain.¹¹⁾

5. Conclusion

In this paper, we have investigated a flat piling of disks in order to define the relation between stress and strain using a numerical experiment and a continuum theory. As a continuum description, we adopted isotropic elasticity theory. In a micro-mechanical approach, we calculated the stress using the mean strain assumption and predicted the Young's modulus and the Poisson's ratio of the pile. The material constants which are measured in the numerical experiments are smaller than those which were predicted using mean strain assumption. In order to obtain a better description, we need to introduce the fluctuation of stress and strain in the pile.

The disorderness of the disk configuration may cause this reduction of stiffness as an aggregate as we can make sure in a pile of disks with a square lattice structure. As a next step, we can introduce an anisotropy of a pile, and see how stress propagation depends on it.

An important questions that should be addressed is the extent to which elasticity theory can be applied to describe unloading of the pile. Preliminary numerical experiments indicate that particle sliding gives rise to irreversible behavior for decreases in gravity larger than ten per cent. The characterization and description of this inelastic behavior will be the subject of a subsequent paper.

- 1) Sarero, D., Reydellet, G., Claudin, P., Clément, E., and Levine, D.: Stress response function of a granular layer: Quantitative comparison between experiments and isotropic elasticity, *Euro. Phys. J. E*, **6** (2001) 169-179
- 2) Vanel, L., Howell, D., Clark, D., Behringer, B.P., and Clément, E.: Effect of construction history on the stress distribution under a sand pile, *Phys. Rev. Lett*, **60** (1999) R5040-5043
- 3) Geng, J., Longhi, E., Behringer, R.P., and Howell, D.W.: Memory in two-dimensional heap experiments, *Phys. Rev. E*, **64** (2001) 060301R
- 4) Cundall, P.A., and Strack, O.D.I.: A discrete numerical model for granular assemblies. *Géotechnique* **29** (1979) 47-65
- 5) The Society of Powder Technology, Japan Eds: Introduction to granular simulation (Sangyo Tosho, Tokyo, 1998) in Japanese. (Funtai simulation Nyumon) Errata by A. Shimosaka : <http://www.ijnet.or.jp/SPTJ/SocPowTec/shusei.html>
- 6) Hayakawa, H.: The distinct element method, in Japanese (unpublished but accessible at <http://ace.phys.h.kyoto-u.ac.jp/hisao/jpapers/dem.ps.gz>)
- 7) Bathurst, R.J. and Rotheburg, L.: Micromechanical aspects of isotropic granular assemblies with linear contact interactions, *J. Applied Mechanics*, **55** (1988) 17
- 8) Bagi, K.: Stress and strain in granular assemblies, *Mechanics of materials*, **22** (1996) 165-177
- 9) Satake, M.: Stress and strain in granular materials, *Powders and Grains 2001* (2001)
- 10) Jenkins, J.T.: Volume change in small strain axisymmetric deformations of a granular material, *Micromechanics of Granular Materials* ed. by M. Satake and J.T.Jenkins, Elsevier Science Publishers (1988) 245
- 11) Jenkins, J.T., and LaRagione, L.: Fluctuation and state variables for random arrays of identical disks, *Powders and Grains 2001*, (2001) 195

Table I. Parameters in our numerical experiments

Diameters of disks	7.6 and 8.0 ($10^{-3}m$)
Thickness of disk	6.0 ($10^{-3}m$)
Density of disk	1.06×10^3 (kg/m^3)
Gravitational Accel.	10 (m/s^2)
Restitution Coef.	0.6
Frictional Coef.	0.4
Normal elastic Coef. (k_n)	1.27×10^4 (N/m)
Tang. elastic Coef. (k_t)	2.54×10^3 (N/m)
Normal viscous Coef. (η_n)	1.00 (kg/s)
Tang. viscous Coef. (η_t)	1.00 (kg/s)
Time step (dt)	3.16×10^{-7} (s)

Shio Inagaki and James T. Jenkins

Fig. 1.

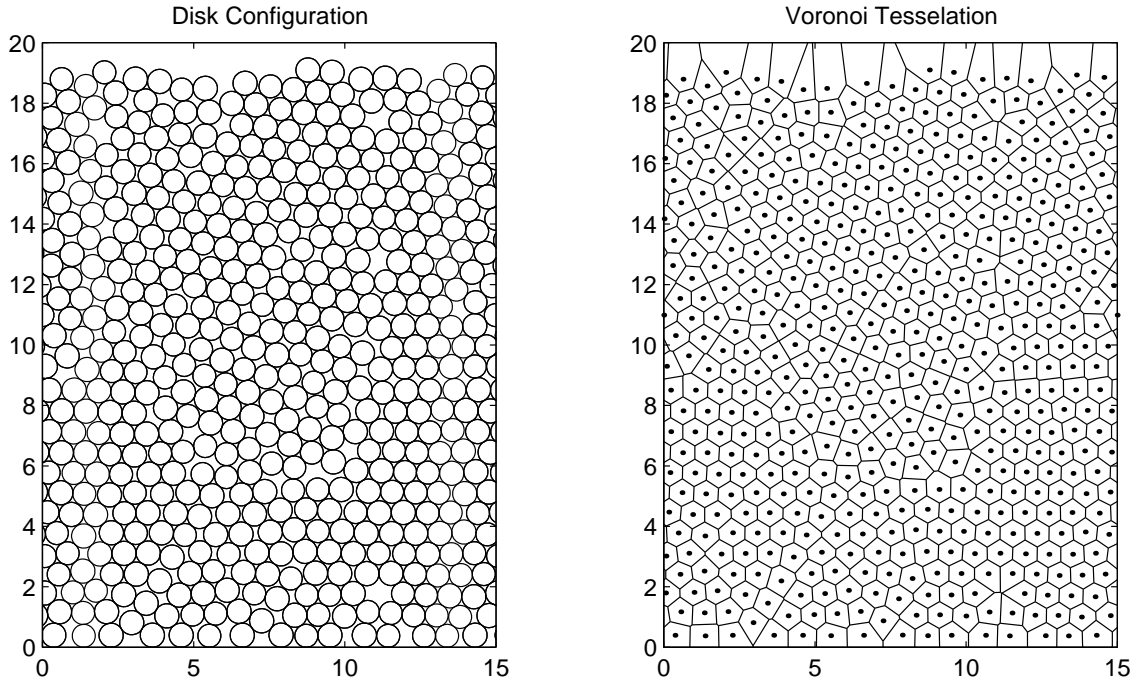
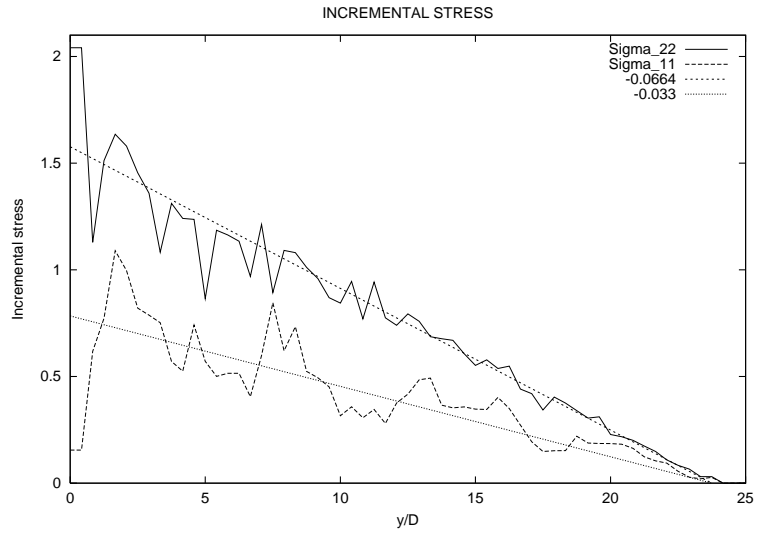


Fig. 2.



Shio Inagaki and James T. Jenkins

Fig. 3.

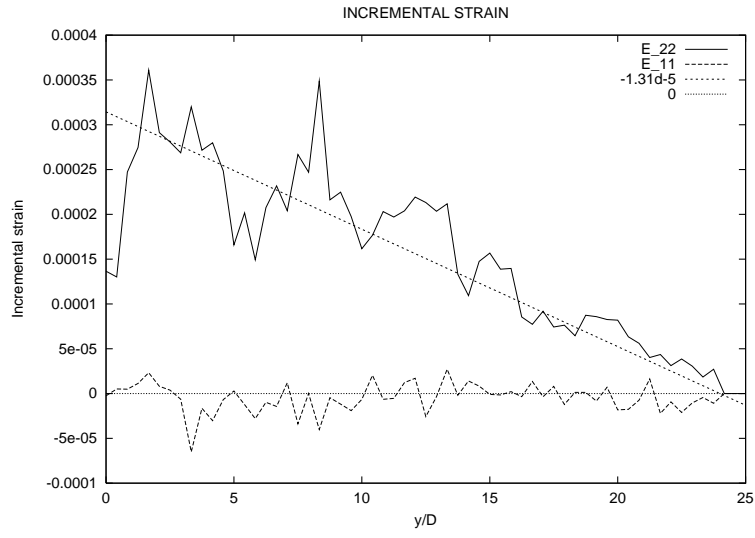
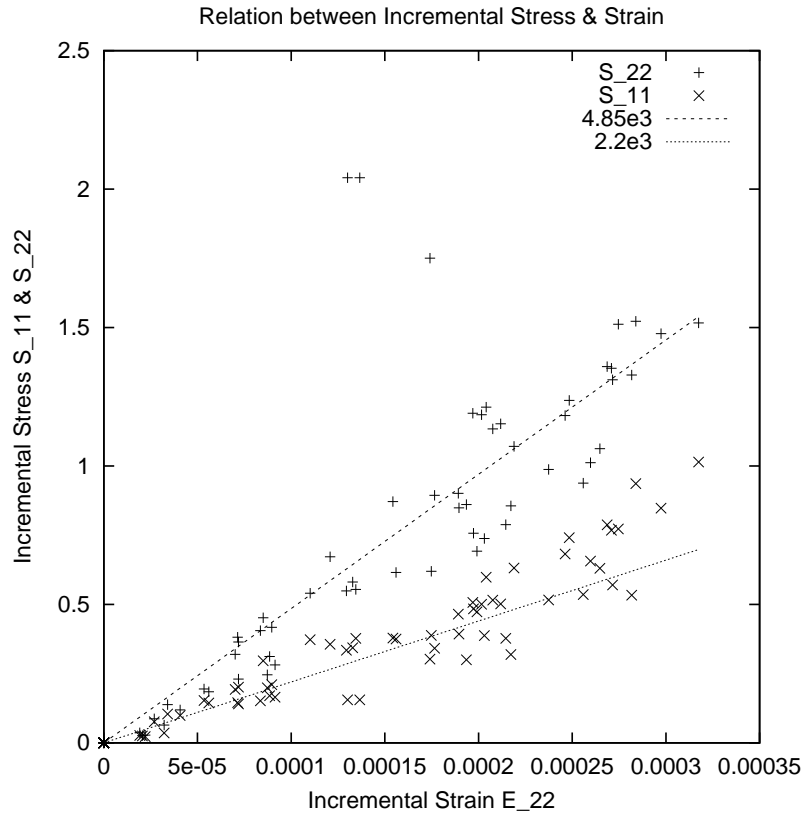


Fig. 4.



Shio Inagaki and James T. Jenkins

Fig. 5.

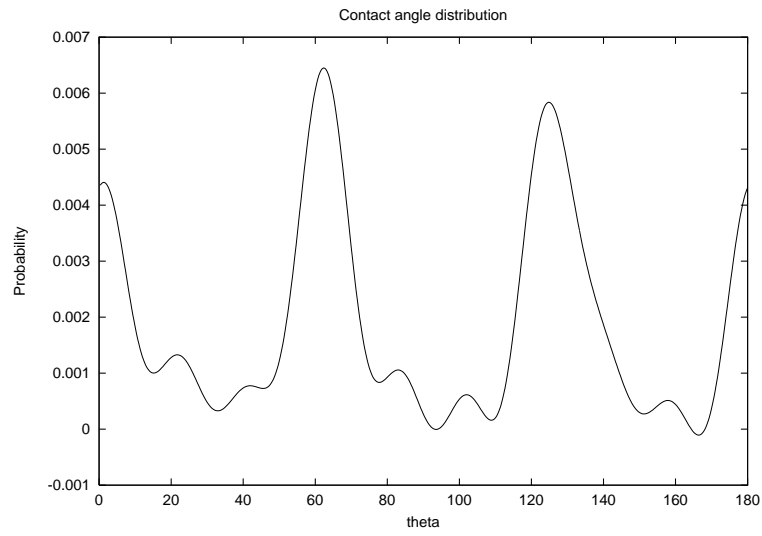
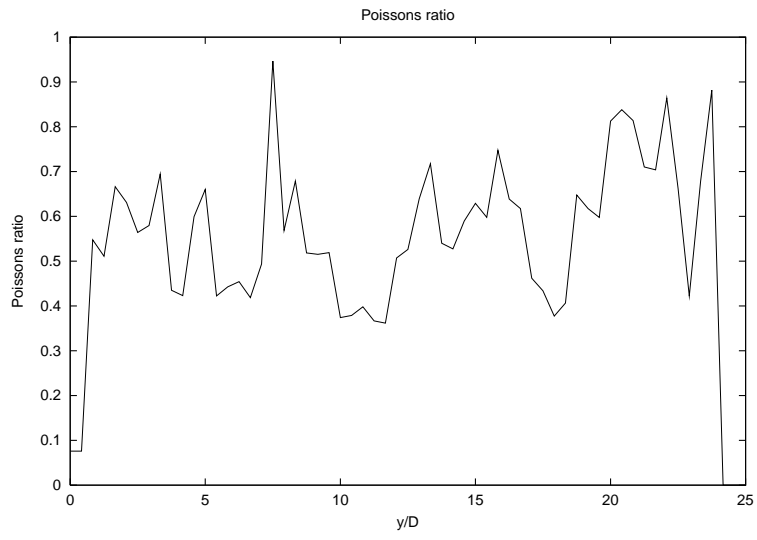


Fig. 6.



Shio Inagaki and James T. Jenkins

Fig. 7.

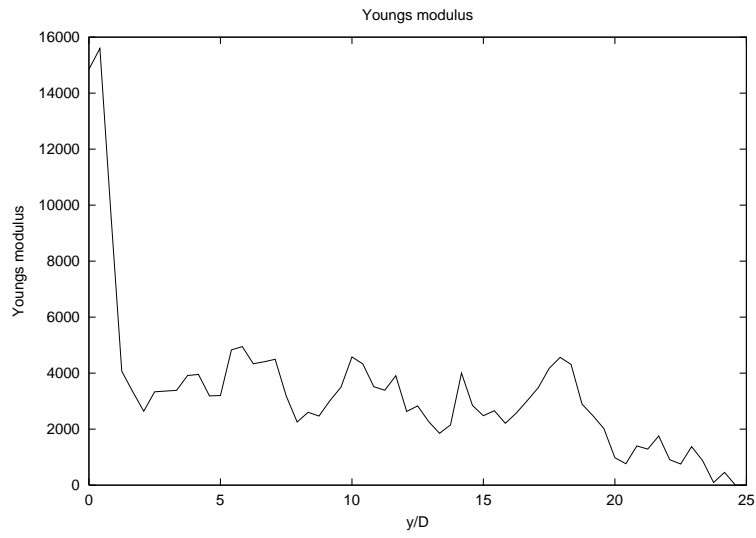


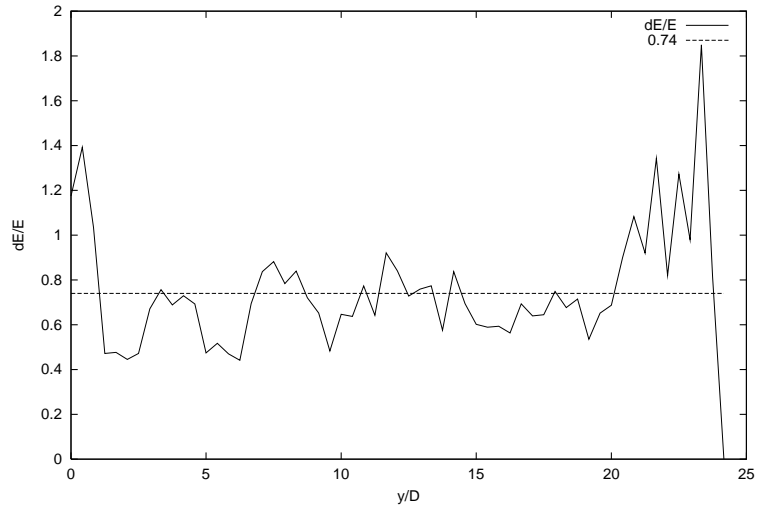
Fig. 8.
Fluctuation of Strain

Figure 1. Left panel: The configuration of disks consisting from 495 disks in a static state. The horizontal boundary is periodic. The diameters of disk is 0.76 *cm* and 0.8 *cm*. Right panel: The lines show Voronoi cells and dots show centers of disks.

Figure 2. The increment of the dimensionless stress versus the height normalized by the maximum diameter (*D*), The inclinations of the straight lines for σ'_{11} and σ'_{22} are -0.0664 and -0.033 respectively. This dimensionless stress, σ' , is converted to the dimensional value, σ , as $\sigma = (\bar{m}g/l) \sigma'$.

Figure 3. The increment of strain versus height normalized by the maximum diameter (*D*). The slopes of the straight lines for E_{11} and E_{22} are 0 and $-1.31 * 10^{-5}$ respectively.

Figure 4. The increments of stress, σ_{xx} and σ_{yy} , versus the increment of strain, E_{yy} . The relation between the increments of stress and strain seems to be linear. The slope of the straight line is $2.2 * 10^3$ (for σ'_{11} (x), and $4.85 * 10^3$ for σ'_{22} (+)).

Figure 5. Probability distribution function of contacts versus contact angle from 0 to π . Three peaks are found $\pi/3, 2\pi/3$ and π . It implies that the packing can be assumed to be almost hexagonal.

Figure 6. Poisson's ratio, versus height normalized by the maximum diameter. This is the ratio of σ_{11} against σ_{22} The mean value is about 0.5.

Figure 7. The dimensionless Young's modulus, E' , versus height normalized by the maximum diameter. It is estimated from eq. (18). The mean value is around $3.6 * 10^3$, and the dimensional value, E , is converted with the relation $E = (\bar{m}g/l) E'$.

Figure 8. The ratio of the fluctuation of E_{22} , ΔE_{22} , to E_{22} versus height normalized by the maximum diameter. The strain fluctuation is almost 74 % of the strain in average except near the surface and the bottom.